==

Response to the Second Referee

==

Reviewer #2:

This article analyses the potential synoptic controls over central China during winter haze pollution episodes by using Lamb-Jenkension method and the NCEP/NCAR FNL operational global analysis data, and further evaluates the effectiveness of emission control to reduce PM2.5 under main synoptic conditions by GEOS-Chem model simulations. They found a substantial contribution of transportation in two synoptic patterns (SW-type and NW-type) and a dominated contribution of local emission sources in other two synoptic conditions (A-type and C-type). These results provide an opportunity to effectively mitigate haze pollution by local emission control actions in coordination with regional collaborative actions according to different synoptic patterns. The topic is of practical significance and the results are reliable. I would suggest for publication after addressing my comments below.

We thank the reviewer for comments, which have been incorporated to improve the manuscript.

1. The present comparison and verification of control simulation results in GEOS-Chem is not enough. It can be further verified by using PM2.5 observation data in a larger region of China or component observations of PM2.5 at some specific sites.

We thank the referee for his/her reading of our manuscript. The comments and suggestions are valuable for us to improve our work.

In order to better evaluate the GEOS-Chem model performances, the spatial distribution of $PM_{2.5}$ concentrations averaged over the four typical heavy pollution processes simulated by the control (CON) simulation are compared with the observations (a total of 633 sites) from Ministry of Ecology and Environment of China (http://www.mee.gov.cn/) (revised Fig. 6). Similar to the underestimation in $PM_{2.5}$ at Jingzhou, the underestimation is on a national scale when compared with the MEE observations, with a bias of -29.3 $\mu g/m^3$, -18.7 $\mu g/m^3$, -39.0 $\mu g/m^3$ and -21.4 $\mu g/m^3$ on average for SW-type, NW-type, A-type and C-type synoptic pattern, respectively (Fig. 6).

We have no observations of the chemical compositions of $PM_{2.5}$. In order to examine the model performances in the $PM_{2.5}$ chemical compositions, we have added Table 4 to review the reported concentrations of $PM_{2.5}$ and the three inorganic salts (sulfate, nitrate and ammonium) in other cities. The contributions of sulfate, nitrate and ammonium are 9.1%-31.9%, 5.7%-32.1% and 5.9%-13.3%, respectively. In the CON simulation, the fractions of each inorganic salt to $PM_{2.5}$ for these four typical heavy pollution processes are shown in revised Fig. S10, which are comparable to the previous observed results (Table 4).

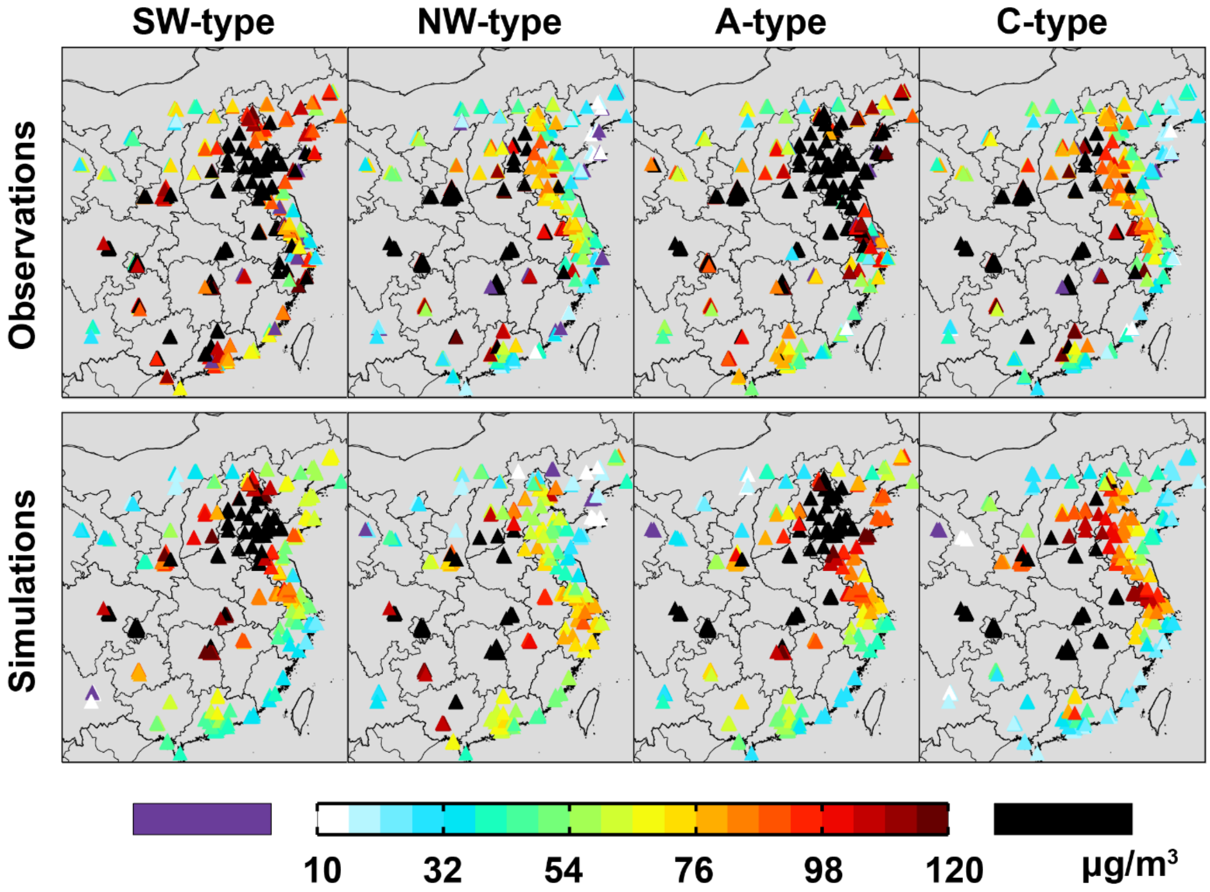

Figure 6 Spatial distribution of observed (top row) and modeled (bottom row, by CON case) $PM_{2.5}$ concentrations (μg/m^3) averaged over four severe pollution episodes controlled by SW-type (first column), NW-type (second column), A-type (third column) and C-type (forth column) synoptic pattern, respectively.

Table 4 The reported concentrations of $PM_{2.5}$ and the three inorganic salts (sulfate, nitrate and ammonium, μg/m^3) in other cities.

References	Site	Time	$PM_{2.5}$	Sulfate	Nitrate	Ammonium
Cao et al., 2012	Beijing	01/03	115.6±46.6	20.0±4.2 (17.3%)	13.1±4.5 (11.3%)	9.4±4.1 (8.1%)
Cao et al., 2012	Qingdao	01/03	134.8±43.0	21.1±7.7 (15.7%)	19.3±9.2 (14.3%)	15.3±5.2 (11.4%)
Cao et al., 2012	Tianjin	01/03	203.1±76.2	32.5±15.1 (16.0%)	25.2±10.3 (12.4%)	22.2±9.8 (10.9%)
Cao et al., 2012	Xi'an	01/03	356.3±118.4	53.8±25.6	29.0±10.0	29.8±11.5

				(15.1%)	(8.1%)	(8.4%)
Cao et al., 2012	Chongqing	01/03	316.6±101.2	60.9±19.6 (19.2%)	18.1±6.4 (5.7%)	28.8±8.9 (9.1%)
Cao et al., 2012	Hangzhou	01/03	177.3±59.5	33.4±16.7 (18.8%)	25.7±14.8 (14.5%)	19.1±10.7 (10.8%)
Cao et al., 2012	Shanghai	01/03	139.4±50.6	21.6±12.3 (15.5%)	17.5±8.7 (12.6%)	14.5±5.9 (10.4%)
Cao et al., 2012	Wuhan	01/03	172.3±67.0	31.4±15.6 (18.2%)	22.2±10.7 (12.9%)	18.4±10.2 (10.7%)
Zhang et al., 2011	Xi’an	03/06-03/07	194.1	35.6 (18.3%)	16.4 (8.4%)	11.4 (5.9%)
Huang et al., 2012	Xi’an	01/06-02/06	235.8±125.1	44.8±31.3 (19.0%)	20.5±14.2 (8.7%)	14.5±10.8 (6.1%)
Wang et al., 2020	Jinan	10/17	104±54	14.4±9.2 (13.8%)	33.4±23.2 (32.1%)	13.0±8.3 (12.5%)
Wang et al., 2020	Shijiazhuang	10/17	152±109	19.3±19.6 (12.7%)	42.8±41.1 (28.2%)	18.2±17.1 (12.0%)
Wang et al., 2020	Wuhan	12/17	117±33	13.6±3.2 (11.6%)	26.6±11.1 (22.7%)	13.1±3.8 (11.2%)
Wang et al., 2016a	Zhengzhou	01/11-02/11	297±160	48±36 (16.2%)	31±19 (10.4%)	21±16 (7.1%)
Wang et al., 2016a	Zhengzhou	01/12-02/12	234±125	23±10 (9.8%)	22±9 (9.4%)	16±5 (6.8%)
Wang et al., 2016a	Zhengzhou	01/13-02/13	337±168	56±39 (16.6%)	39±20 (11.6%)	31±18 (9.2%)
Luo et al., 2018	Zibo	12/06-02/07	224.9±85.4	40.1±19.2 (17.9%)	18.1±9.0 (8.1%)	21.7±10.2 (9.7%)
Wang et al., 2016b	Shanghai	12/11, 12/12, 12/13	73.9±57.5	12.2±9.2 (16.5%)	14.6±12.2 (19.8%)	8.2±6.7 (11.1%)
Xu et al., 2019	Beijing	02/17-03/17	180.5	20.1 (11.1%)	45.6 (25.3%)	22.5 (12.5%)
Xu et al., 2019	Beijing	05/17-09/17	186.7	20.2 (10.8%)	32.4 (17.4%)	17.1 (9.2%)
Xu et al., 2019	Beijing	10/17-11/17	167.5	17.9	44.5	20.9

				(10.7%)	(26.6%)	(12.5%)
Zheng et al., 2016	Beijing	03/10-05/10	65.2±65.1	11.1±10.1 (17.0%)	11.1±11.0 (17.0%)	6.8±6.7 (10.4%)
Zheng et al., 2016	Beijing	07/09-08/09	88.9±39.1	23.0±13.9 (25.9%)	16.2±11.8 (18.2%)	11.8±6.8 (13.3%)
Zheng et al., 2016	Beijing	12/09-02/10	84.0±66.6	8.1±8.3 (9.1%)	8.0±9.6 (9.0%)	5.9±7.1 (6.6%)
Zheng et al., 2016	Guangzhou	11/10	73.3±16.5	16.6±4.0 (22.6%)	5.7±3.8 (7.8%)	6.2±2.0 (8.5%)
Zheng et al., 2016	Shenzhen	12/09	64.6±24.7	20.6±3.5 (31.9%)	4.9±3.5 (7.6%)	4.6±1.0 (7.1%)
Zheng et al., 2016	Wuxi	04/10-05/10	82.1±27.0	12.8±3.8 (15.6%)	9.9±6.3 (12.1%)	7.0±2.0 (8.5%)
Zheng et al., 2016	Jinhua	10/11-11/11	81.9±26.2	18.3±6.7 (22.3%)	12.6±7.0 (15.4%)	10.4±4.1 (12.7%)
Liu et al., 2018	Chongqing	2012-2013	73.5±30.5	19.7±9.6 (26.8%)	6.5±6.2 (8.8%)	6.1±2.7 (8.3%)
Liu et al., 2018	Shanghai	2012-2013	68.4±20.3	13.6±6.4 (19.9%)	11.9±5.0 (17.4%)	5.8±2.1 (8.5%)
Liu et al., 2018	Beijing	2012-2013	71.7±36.0	11.9±8.2 (16.6%)	9.3±7.5 (13.0%)	5.3±2.7 (7.4%)

Reference:

Cao, J.-J., Shen, Z.-X., Chow, J. C., Watson, J. G., Lee, S.-C., Tie, X.-X., Ho, K.-F., Wang, G.-H., and Han, Y.-M.: Winter and Summer $PM_{2.5}$ Chemical Compositions in Fourteen Chinese Cities, Journal of the Air & Waste Management Association, 62, 1214-1226, 10.1080/10962247.2012.701193, 2012.

Huang, W., Cao, J., Tao, Y., Dai, L., Lu, S.-E., Hou, B., Wang, Z., and Zhu, T.: Seasonal Variation of Chemical Species Associated With Short-Term Mortality Effects of $PM_{2.5}$ in Xi'an, a Central City in China, American Journal of Epidemiology, 175, 556-566, 10.1093/aje/kwr342, 2012.

Liu, Z., Gao, W., Yu, Y., Hu, B., Xin, J., Sun, Y., Wang, L., Wang, G., Bi, X., Zhang, G., Xu, H., Cong, Z., He, J., Xu, J., and Wang, Y.: Characteristics of $PM_{2.5}$ mass concentrations and chemical species in urban and background areas of China: emerging results from the CARE-China network, Atmospheric Chemistry and Physics, 18, 8849-8871, 10.5194/acp-18-8849-2018, 2018.

Luo, Y., Zhou, X., Zhang, J., Xiao, Y., Wang, Z., Zhou, Y., and Wang, W.: $PM_{2.5}$ pollution in a petrochemical industry city of northern China: Seasonal variation and source apportionment, Atmospheric Research, 212, 285-295, 10.1016/j.atmosres.2018.05.029, 2018.

Wang, H. L., Qiao, L. P., Lou, S. R., Zhou, M., Ding, A. J., Huang, H. Y., Chen, J. M., Wang, Q., Tao, S., Chen, C. H., Li, L., and Huang, C.: Chemical composition of $PM_{2.5}$ and meteorological impact among three years in urban Shanghai, China, Journal of Cleaner Production, 112, 1302-1311, 10.1016/j.jclepro.2015.04.099, 2016a.

Wang, J., Li, X., Zhang, W., Jiang, N., Zhang, R., and Tang, X.: Secondary $PM_{2.5}$ in Zhengzhou, China: Chemical Species Based on Three Years of Observations, Aerosol and Air Quality Research, 16, 91-104, 10.4209/aaqr.2015.01.0007, 2016b.

Wang, Q., Fang, J., Shi, W., and Dong, X.: Distribution characteristics and policy-related improvements of $PM_{2.5}$ and its components in six Chinese cities, Environmental Pollution, 266, 10.1016/j.envpol.2020.115299, 2020.

Xu, Q., Wang, S., Jiang, J., Bhattarai, N., Li, X., Chang, X., Qiu, X., Zheng, M., Hua, Y., and Hao, J.: Nitrate dominates the chemical composition of $PM_{2.5}$ during haze event in Beijing, China, Science of the Total Environment, 689, 1293-1303, 10.1016/j.scitotenv.2019.06.294, 2019.

Zhang, T., Cao, J. J., Tie, X. X., Shen, Z. X., Liu, S. X., Ding, H., Han, Y. M., Wang, G. H., Ho, K. F., Qiang, J., and Li, W. T.: Water-soluble ions in atmospheric aerosols measured in Xi'an, China: Seasonal variations and sources, Atmospheric Research, 102, 110-119, 10.1016/j.atmosres.2011.06.014, 2011.

Zheng, J., Hu, M., Peng, J., Wu, Z., Kumar, P., Li, M., Wang, Y., and Guo, S.: Spatial distributions and chemical properties of $PM_{2.5}$ based on 21 field campaigns at 17 sites in China, Chemosphere, 159, 480-487, 10.1016/j.chemosphere.2016.06.032, 2016.

2. The novelty of this study need to be further clarified. New understanding or improvement of conclusion and application or in methods should be provided to reflect the general interests of the work rather than the local interests.

In Sect.1, we have further clarified and provided support that significant and new scientific merits are presented in this work. The $PM_{2.5}$ pollution in China has been continuously alleviating since 2013 as the implication of the Air Pollution Prevention and Control Action Plan. However, severe particle pollution still occurs frequently in autumn and winter, which is the major reason restricting the $PM_{2.5}$ to come up to national standard. Currently, how to effectively reduce emissions in autumn and winter is the key to mitigate haze pollution in China. Previous studies have highlighted that different levels of $PM_{2.5}$ pollutions are closely related to the dominant synoptic patterns in different regions, and they attribute the large spatial variability of pollution to the regional transport contributions, not only the different local sources of $PM_{2.5}$. Thus, heavy pollution prevention and control needs to consider the weather situation, otherwise local emission reduction measures would not work well. However, under different synoptic conditions, how to effectively reduce local and regional emissions to control haze pollution is rarely reported. In order to investigate the effectiveness of emission control to reduce $PM_{2.5}$ pollution under various potential synoptic controls, we take the severe particle pollution of winter haze episodes over Central China with transmission-pollution characteristics as an example. This study could provide reference for emission control of severe winter haze pollution under different weather types, and provide basis for regional air quality policy-making.

3. Lines 105-109: several studies have investigated the potential effective emission reduction on ammonia, which should be reviewed here properly.

We have added the review of studies on potential efficiency of ammonia emission reduction in alleviating particulate pollution: "Moreover, current emission reduction policies in China mainly aimed at sulfur dioxide (SO_2) and nitrogen dioxide (NO_2), ignoring the effective emission reduction on ammonia (NH_3), although some modeling works have discussed the effectiveness of ammonia emission reduction for $PM_{2.5}$ mitigations (Liu et al., 2019; Ye et al., 2019; Xu et al., 2019; Bai et al., 2019)."

Bai, Z., Winiwarter, W., Klimont, Z., Velthof, G., Misselbrook, T., Zhao, Z., Jin, X., Oenema, O., Hu, C., and Ma, L.: Further Improvement of Air Quality in China Needs Clear Ammonia Mitigation Target, Environmental Science & Technology, 53, 10542-10544, 10.1021/acs.est.9b04725, 2019.

Liu, M., Huang, X., Song, Y., Tang, J., Cao, J., Zhang, X., Zhang, Q., Wang, S., Xu, T., Kang, L., Cai, X., Zhang, H., Yang, F., Wang, H., Yu, J. Z., Lau, A. K. H., He, L., Huang, X., Duan, L., Ding, A., Xue, L., Gao, J., Liu, B., and Zhu, T.: Ammonia emission control in China would mitigate haze pollution and nitrogen deposition, but worsen acid rain, Proceedings of the National Academy of Sciences of the United States of America, 116, 7760-7765, 10.1073/pnas.1814880116, 2019.

Xu, Z., Liu, M., Zhang, M., Song, Y., Wang, S., Zhang, L., Xu, T., Wang, T., Yan, C., Zhou, T., Sun, Y., Pan, Y., Hu, M., Zheng, M., and Zhu, T.: High efficiency of livestock ammonia emission controls in alleviating particulate nitrate during a severe winter haze episode in northern China, Atmospheric Chemistry and Physics, 19, 5605-5613, 10.5194/acp-19-5605-2019, 2019.

Ye, Z., Guo, X., Cheng, L., Cheng, S., Chen, D., Wang, W., and Liu, B.: Reducing $PM_{2.5}$ and secondary inorganic aerosols by agricultural ammonia emission mitigation within the Beijing-Tianjin-Hebei region, China, Atmospheric Environment, 219, 10.1016/j.atmosenv.2019.116989, 2019.

4. In Section 3.2, the mechanisms of heavy particle pollution caused by these four potential synoptic controls should be briefly discussed when describe characteristics of each synoptic pattern.

We have briefly discussed the mechanisms of heavy particle pollution caused by the four PSCs in the revised Section 3.2, when describe characteristics of each synoptic pattern:

"SW-type circulation is the predominant PSC of severe $PM_{2.5}$ pollution episodes. The circulation at 500 hPa is relatively flat and the whole East Asia region is affected by the westerly flow (Fig. S6a). Westerly belt fluctuates greatly at 700 hPa and there are two ridges and a southwest trough in the middle latitudes of Asia (Fig. S7a). Jingzhou is located in the front of a trough, prevailing the weak southwest airflow. At 850 hPa, the cold high pressure center is formed in Xinjiang of China. Warm low pressure appears in the low latitude area and weak high pressure appears in the East China Sea (Fig. 3a). In combination with the surface field, a high-low-high saddle like field forms from west to east (Fig. 4a). Such synoptic type is also the dominant weather system of eastern China (Shu et al., 2017; Yang et al., 2018). Jingzhou is located in the back of Bohai-northeast high pressure and the front of southwest warm low pressure. Thus it is affected by the southerly airflow, which could be conducive to the transport of air pollutants formed over southern China to Central China. Associated with small local surface wind speed (< 3 m/s) at Jingzhou, the dispersion of local and transported pollutants is inhibited.

NW-type circulation mainly occurs in the early winter (December and January). This synoptic pattern is also reported as one of the main types to affect the aerosol distributions over eastern China (Zheng et al., 2015). Circulation at 500 hPa is controlled by one trough and one ridge, with the weak ridge located in the northwest of China and the shallow trough located in the northeast of China (Fig. S6b). The whole East Asia is affected by the westerly current. The trough and ridge at 700 hPa are deepened. Jingzhou is located at the bottom of the shallow trough, prevailing the west-northwest airflow, affected by the flow around the plateau (Fig. S7b). At 850 hPa, the cold high pressure center is formed in Xinjiang, and Jingzhou is affected by the northerly airflow, due to being in the front of the high pressure (Fig. 3b). For the sea level pressure, the cold high pressure is located in the west of Mongolia and Xinjiang of China (Fig. 4b). Jingzhou is located at the region with weak fluctuation in the front of the high pressure, and the surface wind speed is smaller than 2 m/s. The haze episodes induced by NW-type synoptic pattern is similar to the transmission-accumulation pollution caused by SW-type, but the transmission path is from Northern China to Central China.

A-type circulation also mainly occurs in the early winter. The high-altitude circulation field is controlled by one trough and one ridge (Fig. S6c and S7c). East Asia is affected by west-northwest air flow, and the SLP is controlled by a huge high pressure, with the center located in the southwest of Baikal Lake (Fig. 4c). A surface high pressure favors the accumulation of air pollutants, especially over the regions of high pressure center (Leung et al., 2018). Jingzhou is in the sparse pressure field in front of the high pressure (Fig. 3c and 4c), with an average surface wind speed of ~1.3 m/s. The uniform west-northwest air flow at high altitude would lead to the low water vapor content and less cloud amount, which is conducive to radiation cooling at night. In addition, due to the weak high pressure ridge in the north, it is not conducive to the eastward and southward movement of cold air, leading to the stable weather situation and thus severe haze pollution at Jingzhou. This type is also responsible for most of the severe particulate pollution days in the BTH and YRD regions (Li et al., 2019).

C-type circulation mainly occurs in late winter and early spring, when the relative humidity is large with an average value of 74%. East Asia is controlled by the straight westerly flow, and the southwest shallow trough is obvious at 500 hPa (Fig. S6d). Additionally, the West Pacific subtropical high extends to the west, Central China is affected by the southwest flow. Southwest trough is deepened at 700 hPa, and Jingzhou is located in front of the trough and controlled by the southwest airflow (Fig. S7d). High pressure at the south of Xinjiang and the north of Plateau is strengthened at 850 hPa, and the southwest low pressure center is formed (Fig. 3d). Jingzhou is located in the low pressure system on the SLP field (Fig. 4d), with small surface wind speed (0-3 m/s). Together with the large relative humidity, which can promote the hygroscopic growth of particulate matter (Twohy et al., 2009; Zheng et al., 2015), the haze pollution is persistent and serious at Jingzhou. The impact of low-pressure systems on winter heavy air pollution have also been reported in the northwest Sichuan Basin (Ning et al., 2018)."

5. Lines 294-296: Why the four pollution episodes are selected?

We have explained in the revised sentences: "In order to reduce the simulation cost, the continuous four severe haze episodes occurred during November, 2013-February, 2014 are selected. These four haze episodes are controlled by the synoptic pattern of SW-type (18-25 November, 2013), NW-type (19-26 December, 2013), A-type (14-21 January, 2014) and C-type (26 January - 2 February, 2014), respectively."

6. Lines 304-308: The model control simulation is compared to PM2.5 observations at just one site (Jingzhou). Current comparison is insufficient to demonstrate the modeling performance.

In order to better evaluate the GEOS-Chem model performances, the spatial distribution of $PM_{2.5}$ concentrations averaged over the four typical heavy pollution processes simulated by the control (CON) simulation are compared with the observations (a total of 633 sites) from Ministry of Ecology and Environment of China (http://www.mee.gov.cn/) (revised Fig. 6). Please see details in the response of comment#1.

7. Line 308-311: Model biases are generally attributed to resolution, emission errors, meteorology and chemical mechanism without statistical results of further sensitivity simulations. Be careful to discuss the model deviation.

In order to explain the causes of the model discrepancy, we have added Table S3 to show the observed (modeled) meteorological conditions averaged over these four pollution episodes controlled by SW-type, NW-type, A-type and C-type synoptic pattern, respectively. There is an overestimate in temperature and wind speed and an underestimate in humidity, which can partly contribute to the underestimation of modeled $PM_{2.5}$ concentrations. In addition, anthropogenic emissions for $PM_{2.5}$ precursors used here are for the year 2017 over Central China from SEEA inventory (revised Table S4). From 2013 to 2017, anthropogenic NO_x, SO_2, and primary $PM_{2.5}$ emissions in Central China have declined substantially (revised Table S4), due to the implementation of stringent emission control measures for the 12th-13th Five-Year Plans (Zheng et al., 2018). The anthropogenic emissions biases may affect our simulations and $PM_{2.5}$ attribution results to some extent. Additionally, the underestimation is on a national scale when compared with the MEE observations, with a bias of -29.3 μg/m^3, -18.7 μg/m^3, -39.0 μg/m^3 and -21.4 μg/m^3 on average for SW-type, NW-type, A-type and C-type synoptic pattern, respectively (revised Fig. 6, see figure in the response of comment#1). The national negative biases may be also attributed to insufficient resolution of the model (Yan et al., 2014) and imperfect chemical mechanisms (Yan et al., 2019).

Table S3. The observed (modeled) meteorological conditions at Jingzhou averaged over these four pollution episodes controlled by SW-type, NW-type, A-type and C-type synoptic pattern, respectively.

PSC	Temperature (°C)	Humidity (%)	Pressure (kpa)	Wind speed (m/s)
SW	11.79 (12.96)	75.33 (69.25)	1018.33 (1024.06)	2.13 (3.09)
NW	3.61 (6.34)	71.16 (62.78)	1027.53 (1031.53)	1.44 (2.45)
A	5.81 (7.52)	64.96 (60.38)	1026.63 (1028.66)	1.45 (2.27)
C	9.60 (13.08)	78.10 (71.40)	1011.48 (1014.24)	1.88 (3.11)

Table S4. The emission amount of $PM_{2.5}$ precursors over Central China calculated from SEEA (for the year 2017) and MEIC (for the years of 2013, 2014 and 2017) inventory (unit: 10^4 ton).

Category	SO_2	NO_X	NH_3	$PM_{2.5}$	CO	BC	OC	VOCs
SEEA (2017)	48.4	94.0	54.6	26.4	553.8	6.2	12.9	117.2
MEIC (2017)	52.0	70.4	57.5	35.2	629.2	6.8	11.7	116.4
MEIC (2013)	173.3	98.4	62.4	54.5	836.5	9.2	16.7	116.6
MEIC (2014)	97.0	80.0	61.1	46.8	744.2	8.3	15.3	116.4

8. Line 337: PSC -> PSCs

Modified.

9. Line 359: The transportation of air pollutants from the south makes the proportion of the three inorganic salts (45.7%) in Jingzhou area the smallest. Consider revising it like: The transport of air pollutants from the south leads to the smallest proportion of the three inorganic salts (45.7%) in Jingzhou.

Modified.

10. Line 482: remove potential synoptic controls or (PSC)

Modified.

11. Line 494: contribute 82%/85% of PM2.5. Consider revising it like: dominate the contribution (82%/85%) to PM2.5.

Modified.